Surface Acidic Properties of A HMCM-22 Zeolite: Collidine Poisoning and Hydrocarbon Adsorption Studies

Hongwei Du[†,‡] and David H. Olson*[,†]

University of Pennsylvania, Department of Chemical Engineering, 311A Towne Building, 220 S. 33rd Street, Philadelphia, Pennsylvania 19104

Received: August 27, 2001; In Final Form: October 30, 2001

The total and external surface acidic properties of a HMCM-22 ($SiO_2/Al_2O_3 = 33$) zeolite have been studied by temperature-programmed ammonia desorption (TPAD) and temperature-programmed collidine desorption (TPCD), respectively. Ammonia TPD results indicate that the Brønsted acid sites in HMCM-22(33) have a relatively uniform acid strength, and most of them are strong. Collidine TPD shows that the Brønsted acid sites on the external surface accessible to collidine accounts for 12% of the total Brønsted acid sites. Strong Brønsted acid sites are present on the zeolite surface as indicated by the collidine desorption at high temperature. The two distinct desorption regions in the low- and high-temperature ranges shown in the collidine TPD curve are ascribed to collidine physisorption and chemisorption, respectively. Chemisorbed collidine on the zeolite surface does not influence the sorption rate of 3-methylpentane, indicating that it does not block 10-ring pore mouth openings. This means that collidine can selectively poison the Brønsted acid sites on the MCM-22 surface without influencing the access to intracrystalline acid sites. It is also found that collidine poisoning on the MCM-22 surface does not influence ethylbenzene sorption rate, indicating that the very low activity of collidine-poisoned HMCM-22 zeolite, in the benzene alkylation with ethylene reaction, is not caused by zeolite pore mouth blocking. This supports the external surface reaction mechanism proposed by Cheng et al.

Introduction

MCM-22 zeolite, having MWW topology, is one of the most interesting of the recent new zeolites.[1] It has unique structural features, possessing two independent, 10-ring defining pore systems. One pore system consists of two-dimensional, sinusoidal, intersecting 10-ring channels with an elliptical ring cross section of 0.41 × 0.51 nm. The other system possesses large cylindrical supercages whose diameter is defined by a 12-membered ring (12-MR), having interior free dimensions of 0.71 × 0.71 × 1.82 nm. The 12-MR supercages are accessed by 0.45 × 0.55 nm, 10-membered ring windows. Half 12-MR cages (0.71 × 0.71 × 0.92 nm) form large adsorption pockets on the external [001] crystal surfaces. Typically, MCM-22 zeolite crystallizes as thin platelets, endowing this materials with large external surface area dominated by these [001] surfaces.[2]

MCM-22 zeolites show high thermal stability, large sorption capacity and high surface area rendering these materials very interesting for catalysis.[3] It has been shown to be a catalyst in many Brønsted acid-catalyzed reactions, e.g., catalytic cracking, olefin isomerization, alkylation of aromatics, and the conversion of paraffins to olefins and aromatics.[4,5] The product selectivities of MCM-22 in the above reactions frequently show a combination of the selectivities of 12-MR large pore zeolites and 10-MR medium pore zeolites, reflecting the significant contribution of external surface acid sites. The large 12-MR cages accessible through 10-ring windows make MCM-22 particularly useful in the reactions with bulky transition-state intermediates, which are normally sterically constrained in medium pore zeolites such as ZSM-5. Yashima et al. reported that disproportionation of toluene proceeds facilely because the large cages of MCM-22 zeolite easily accommodate the large di-toluene reaction intermediate.[6] In this reaction, *para*-xylene forms as a primary product due to the "product selectivity" caused by the steric restriction of the 10-MR windows on the larger *meta*- and *ortho*-xylene molecules.[6] The *para*-xylene initially formed may be subsequently isomerized to *m*- and *o*-xylene in the 10-MR channels and on the external surface. It has been found that decreasing the catalyst contact time, poisoning the external surface and moderate dealumination treatment can considerably suppress the isomerization reactions leading to higher para selectivity.[6]

The external surface of MCM-22 zeolite is composed of two parts. The majority of the external surface area is on the [001] crystal faces containing the 9 Å deep, 12-ring diameter surface pockets (Figure 1).[7] A small fraction of the external surface area is on the thin crystal edges, normal to the [001] surface; these surfaces contain the 10-MR pore openings accessing the intracrystalline regions. On the external surface, tetracoordinated aluminum atoms fully connected to the framework may exist, particularly in the deep surface pockets, and these could be the source of high acid activity. Indeed, even though the intracrystalline pore regions are accessed via 10-rings, there have been several reports showing that the catalytic shape selectivity is intermediate between that of 10- and 12-ring zeolites, indicating that external surface acid sites are contributing to the catalytic conversion.[8,9] In some reactions, the external surface acidity plays a dominate role. For example, the benzene alkylation with ethylene reaction has been postulated to occur essentially

* Corresponding author. E-mail: dholson@seas.upenn.edu. Fax 215-573-2093.

† University of Pennsylvania.

‡ Present address: Department of Chemical Engineering, Northwestern University, 2145 Sheridan Road, E136 Evanston, IL 60208.

10.1021/jp013310s CCC: $22.00
Published on Web 12/19/2001

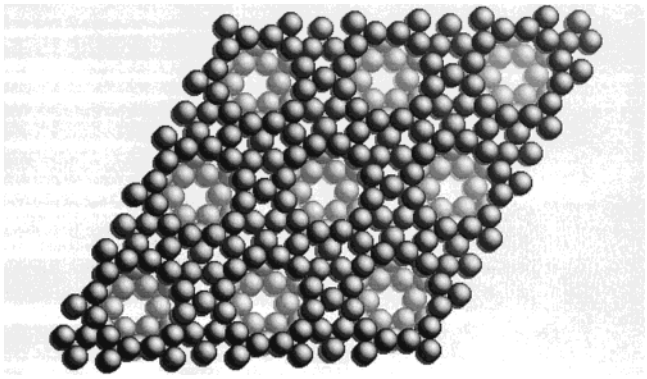

Figure 1. [001] surface of MCM-22 zeolite showing external surface pockets. Six rings are at the bottom of the pocket.

completely on the external surface of MCM-22 zeolite.[10] This process has been commercialized by Mobil Technology Company using MCM-22 zeolite as the catalyst.

Undoubtedly, the external surface acidity of MCM-22 zeolite plays a very important role in many catalytic reactions. So far, much work has been done on the study of structural, adsorptive, and catalytic properties of MCM-22 zeolite.[11−13] By comparison, there has been very limited study of the external surface acidity. Sastre et al. reported a computer simulation study on this subject.[14] Also, for MCM-22 zeolite, it is of importance to distinguish the external surface acidity from intracrystalline acidity. A common way to differentiate these two sources is to selectively poison the outer surface Brønsted acid sites by chemisorbing bulky base molecules. For instance, for 10-MR medium pore zeolites, 2,4,6-trimethylpyridine (γ-collidine) with a 0.62×0.56 nm cross section is commonly used. Page et al. reported that after the external acid sites were poisoned by γ-collidine, the selectivity of HZSM-23 catalyst for linear hydrocarbon production from lower olefins improved.[15] The side reactions were inhibited due to the deactivation of the external surface acid sites. Heck et al. reported collidine-poisoned HZSM-35 zeolite as a more selective catalyst than the unpoisoned zeolite for converting ethylene to isobutylene; this was attributed to the deactivation of external surface Brønsted acid sites.[16] However, collidine poisoning sometimes has the undesired effect of causing pore mouth blockage. Fota et al. observed 10-MR pore blocking of HZSM-5 zeolite after being poisoned by collidine, hindering the diffusion of ethylene or methanol into 10-MR channels.[17] Cheng et al. reported using collidine-poisoned HMCM-22 in differentiating external surface acid activity from intracrystalline acid activity in the alkylation of benzene with ethylene reaction.[10] However, to date there has been no literature reporting the influence of collidine poisoning on MCM-22 pore openings, leaving the understanding of collidine poisoning in question.

In this paper, the surface acidic properties of MCM-22 zeolite as well as the influence of collidine poisoning on 10-ring pore openings were investigated. Employing temperature-programmed desorption of collidine, the Brønsted acid amount and Brønsted acid strength distribution on the external surface were studied. The influence of collidine poisoning on MCM-22 zeolite 10-ring pore openings was examined via hydrocarbon adsorption rate experiments. Collidine poisoning conditions and their affects on MCM-22 adsorptive properties have been investigated.

Experimental Section

Zeolite Sample Preparation. As-synthesized MCM-22 zeolite was provided by Mobil Technology Company. H-form MCM-22(33) zeolite was obtained by program heating the as-synthesized MCM-22, in flowing dry nitrogen, to 540 °C, then holding at 540 °C for 3 h, followed by program heating from 300 to 540 °C, in dry air, and holding at 540 °C for 3 h. The product was ion-exchanged 3 times at 80 °C with 0.5N NH_4Cl aqueous solution and then calcined at 550 °C in air for 3 h. The resulting HMCM-22(33), white in color, was used primarily for the adsorption studies. NH_4MCM-22 was obtained by ion exchanging HMCM-22(33) at room temperature with 1M NH_4-Cl aqueous solution whose pH value was preadjusted to 8.9 with NH_4OH solution. The resulting mixture was filtered and then mixed with water under stirring, forming a zeolite-water slurry. The resultant slurry was further heated at boiling for half an hour to remove excess ammonia, followed by filtration and drying. The obtained NH_4MCM-22 was used for the ammonia TPD study.

Characterization. Powder X-ray diffraction (XRD) was performed on computer controlled Rigaku Geigerflex diffractometer equipped with a graphite mono-chrometer and using CuKα radiation. Crystal size and morphology were observed using transmission electron microscopy. The samples were prepared for TEM analysis by dispersing and spreading on a carbon coated copper grid. They were examined at 200 kV in a JEOL 2010 TEM equipped with a bottom mounted Gatan CCD camera.

Temperature-programmed desorption of ammonia and collidine were carried out gravimetrically on a computer controlled TA51 electrobalance and Metrom 614 Impulsomat, 632 pH meter and 655 Dosimat titration system; the titration method developed by Kerr was used.[18] For ammonia TPD, about 20 mg NH_4MCM-22 zeolite was placed on the platinum electrobalance sample pan. NH_3−TPD profile was recorded from ambient temperature to 800 °C, at a heating rate of 10 °C/min and with a 100 cm^3/min oxygen-free helium flow. For the collidine TPD, HMCM-22(33) zeolite was placed onto the sample pan and pretreated at 500 °C in dry nitrogen, followed by cooling to the room temperature in dry nitrogen. Collidine vapor carried by nitrogen gas was passed over HMCM-22(33) zeolite until the sample reached constant weight. The TPCD profile was recorded from ambient temperature to 900 °C at a heating rate of 10 °C/min. The base was titrated as described above.

Adsorption measurements were made using a computer controlled thermogravimetric balance consisting of a TA51 electrobalance and associated TA-2000/PC control system. This one atmosphere, gas flow through electrobalance system was controlled via Macintosh based LabView control software, Kinetic Systems Interface, mass flow controllers and Eurotherm temperature controller. The samples were calcined at 500 °C for 3 h in dry N_2 prior to the sorption measurement.

Results and Discussions

Physicochemical Properties of HMCM-22(33). The X-ray diffraction pattern of the calcined HMCM-22(33) is shown in Figure 2. It agrees well with the literature data.[1] No diffraction peaks due to other crystalline phases were observed although MTW or MFI zeolites often coexist with MCM-22 zeolite. As can be seen from the TEM photograph shown in Figure 3, MCM-22 zeolite crystallites show hexagonal platelet morphology with an average diameter of 150 nm.

Total Acidity. The total Brønsted acidity of HMCM-22(33) was measured by temperature-programmed ammonia desorption (Figure 4). The total amount of ammonia desorbed from this NH_4MCM-22 is 0.93 mmol/g, corresponding to a SiO_2/Al_2O_3 ratio of 33. The TPAD dMeq/dT profile (Figure 4) shows a

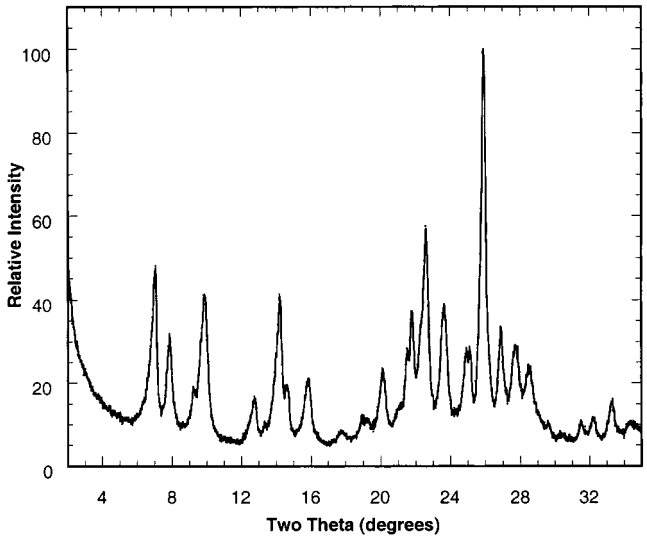

Figure 2. X-ray diffraction pattern for HMCM-22(33), CuKα radiation.

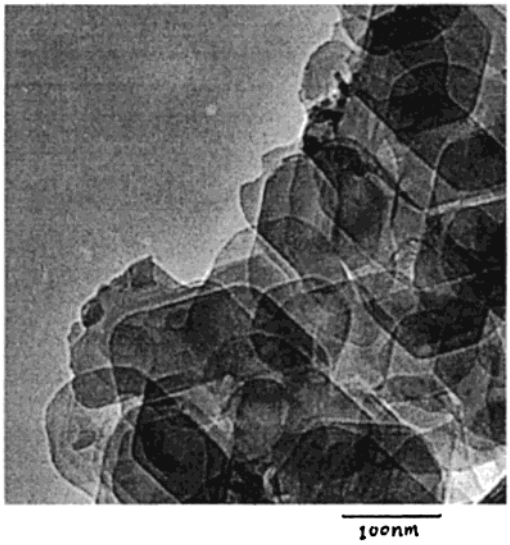

Figure 3. TEM photograph of MCM-22 zeolite.

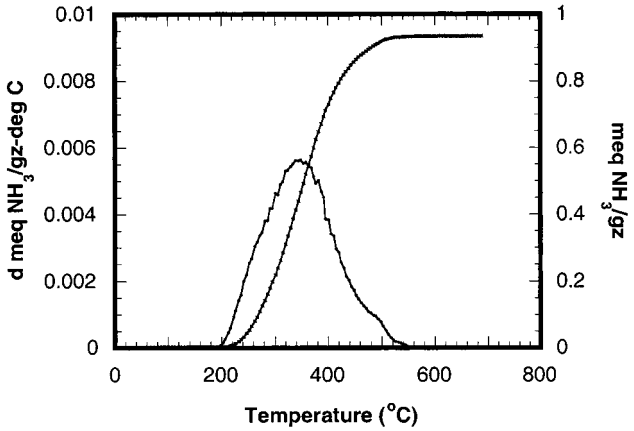

Figure 4. Temperature-programmed desorption of ammonia from NH_4-MCM-22(33). (a) Titration curve, meq NH_3/gz vs *T* (upper curve). (b) Derivative curve, d(meq NH_3/gz)/d*T* vs *T* (lower curve).

single dMeq/d*T* desorption peak with a 150 °C width at half-maximum intensity, indicating a relatively uniform acid strength of the Brønsted acid sites. The peak maximum at about 340 °C indicates that most of the Brønsted acid sites are strong. The derivative TPAD curve for NH_4MCM-22(33) is compared with

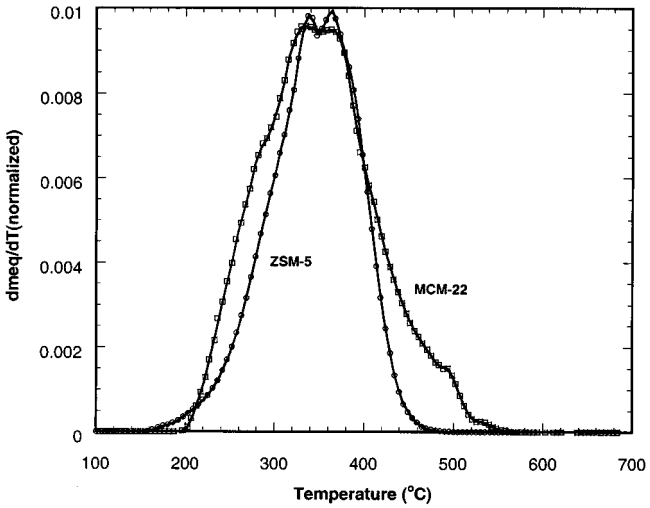

Figure 5. Ammonia desorption derivative curves for (a) NH_4ZSM-5(72) (○) and (b) NH_4MCM-22(33) (□). The derivative values are normalized to an arbitrary maximum value of 0.01.

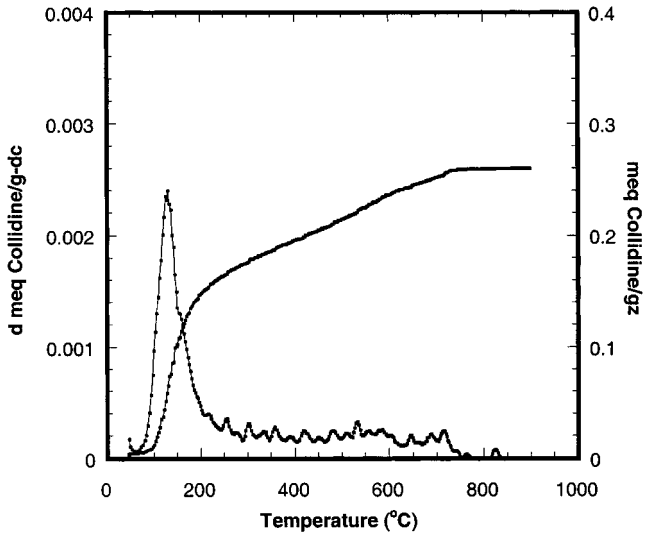

Figure 6. Temperature-programmed desorption of collidine from HMCM-22(33). (a) Titration curve, meq collidine/gz (upper-right curve). (b) Derivative curve, d(meq collidine/gz)/d*T* vs *T* (lower-left curve).

the corresponding curve for a NH_4ZSM-5(72) having uniform, strong acid sites (Figure 5).

External Surface Acidity. The external surface acidic properties of HMCM-22(33) were studied by temperature-programmed desorption of collidine (TPCD). Collidine-poisoned HMCM-22(33) used for the TPCD study was prepared as follows: HMCM-22(33) zeolite was pretreated at 500 °C for 3 h in flowing dry nitrogen and then cooled to room temperature. Nitrogen gas, bubbled through a collidine saturator, was passed over the zeolite sample until collidine adsorption reached a constant value. The sample was then flushed with pure nitrogen at 45 °C until no further weight loss was observed. As can be seen from the collidine desorption curve shown in Figure 6, two distinct desorption steps were observed: one in the 45−200 °C range and the other in the 200−750 °C range. The first desorption peak, in the low-temperature region, is due to collidine weakly adsorbed on the zeolite surface. This low-temperature desorption step is assigned to physisorbed collidine on non-Brønsted acid sites and/or other weak adsorption sites over the zeolite surface as will be verified later. The second

desorption step at the higher-temperature range is due to the strong collidine interaction with the external surface. Collidine is a strong base and is capable of strong chemi-interaction with Brønsted acid sites. The second desorption step at high-temperature range is therefore attributed to the desorption of collidine from external Brønsted acid sites. The amount of the Brønsted acid sites on the external surface accessible to collidine is 0.108 mmol/g, accounting for 12% of the total Brønsted acidity (0.93 mmol/g) as measured by TPAD. The broad chemisorption region (200−750 °C) indicates that Brønsted acid sites on the external surface have a wide range of interaction energies with collidine. The lower-temperature region desorption in the chemisorption range may indicate the presence of steric constraints that weaken the interaction between collidine and the strong Brønsted acid sites located at less accessible positions, such as the bottom of the surface pockets. However, the strong Brønsted acid sites are clearly indicated by the collidine desorbed at high temperature (up to 750 °C). Indeed, the external surface of MCM-22 zeolite has been found to participate in strong Brønsted acid-catalyzed reactions such as *n*-heptane cracking reaction.[19] Also, the MCM-22 external surface are found to be active in many other catalytic reactions such as xylene isomerization, benzene alkylation with propylene, etc.[20,21] Xylene isomerization is a fast reaction and can take place with low catalyst acidity.[22] Benzene alkylation with propylene usually occurs on moderate to strong Brønsted acid sites.[23]

As shown in the collidine dMeq/dT TPD profile (Figure 6), in the physisorption region, one desorption peak appears at 135 °C and ends at 200 °C. This means that with a 200 °C treatment physisorbed collidine can be removed from zeolite surface. The interaction between physisorbed collidine and the MCM-22 external surface will be discussed later.

Effect of Collidine Poisoning on 10-Ring Pore Openings. As mentioned earlier, it is of importance to know if collidine molecules adsorbed on the external surface of MCM-22 surface block zeolite pore openings. We have tested this by measuring the effect of collidine on the intracrystalline adsorption rate of HMCM-22 zeolite. If the 10-ring pore mouth openings are blocked or partially blocked by collidine molecules, the hydrocarbon sorption rate will be decreased. The following comparison adsorption experiments were done with two HMCM-22(33) samples: one collidine-free HMCM-22(33) and the other collidine-poisoned HMCM-22(33), denoted as C−HMCM-22-(33). The latter was prepared by heating collidine-sorbed HMCM-22(33) at 200 °C until no further weight loss was observed. This treatment removes physisorbed collidine, leaving chemisorbed collidine on the C−HMCM-22(33) sample, as indicated by the collidine dMeq/d*T* desorption curve shown in Figure 6. The singly branched hydrocarbon, 3-methylpentane was chosen as the adsorbate probe. The adsorption measurements were done under identical experimental conditions for the two samples: 30 °C and 35 Torr 3-methylpentane. As can be seen from Figure 7, the sorption rate of 3-methylpentane on C−HMCM-22(33) is essentially the same as that on the parent HMCM-22(33), indicating that chemisorbed collidine on the zeolite surface does not block 10-ring pore openings. This shows that collidine can selectively poison the Brønsted acid sites on the external surface without affecting access to the internal acid sites. These results also indicate that there are no strong Brønsted acid sites present in the 10-ring pore mouth area, which otherwise would cause collidine induced pore-mouth blockage. From this, we conclude that most of the Brønsted acid sites on the MCM-22 external surface are located in the external pockets area.

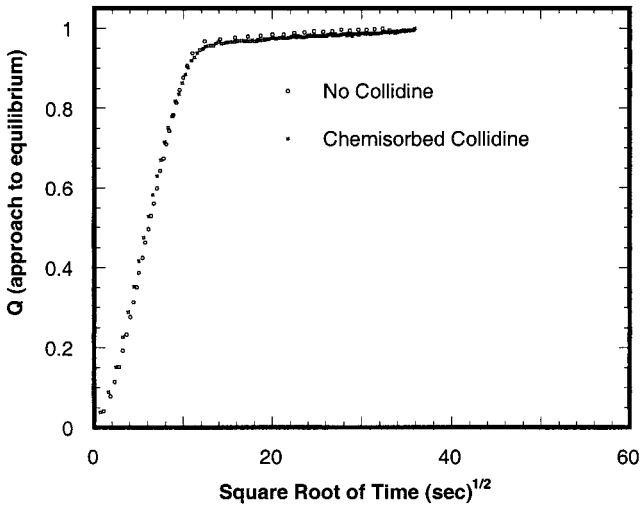

Figure 7. 3-Methylpentane sorption on (a) HMCM-22(33), no collidine (○), and (b) C−MCM-22(33), with chemisorbed collidine (□), plotted as *Q*(approach to equilibrium) as a function of the square root of time ($s^{1/2}$). *Q*(∞) values for these two adsorbents are 98.8 and 76.5 mg/g ash, respectively.

As can be seen from Figure 6, collidine chemisorbed on the external surface starts to desorb at about 200 °C. Thus, when studying external surface acidity using collidine-poisoned HMCM-22, the purge and/or reaction temperature should not exceed 200 °C. At temperatures above ∼200 °C, chemisorbed collidine may be desorbed from Brønsted acid sites causing the incomplete poisoning of surface acidity.

Effect of Physisorbed Collidine on 10-Ring Pore Openings. The results above show that collidine molecules chemisorbed on the external surface are located primarily in the external pockets rather than on the 10-ring pore mouths. It is also of interest to know where the physisorbed collidine molecules are located and if they affect the pore mouth entrances of MCM-22 zeolite. This becomes especially important for reactions carried out at lower temperatures, e.g., below 200 °C, where physisorbed collidine is present. In the patent and scientific literature, zeolite surface poisoning is usually done by adding collidine together with reactants to the reaction system without further treatment to remove physisorbed collidine. These physisorbed collidine molecules may stay on the zeolite if the reaction temperature is lower than 200 °C. To examine the effect of the physisorbed collidine, comparison sorption experiments were done with HMCM-22(33) zeolite containing chemisorbed collidine and HMCM-22(33) zeolite containing both chemisorbed plus physisorbed collidine. The former sample, denoted as C−HMCM-22(33), was prepared as indicated above. The later sample, denoted as P−HMCM-22(33), was prepared by flushing collidine-sorbed HMCM-22(33) at 45 °C in dry N_2 until the zeolite weight was constant. For this sample, both chemisorbed collidine and physisorbed collidine were present. As can be seen from the adsorption results shown in Figure 8, the sorption rate of 3-methylpentane on P−HMCM-22(33) is much lower than that on C−HMCM-22(33), indicating that physisorbed collidine molecules are blocking zeolite pore entrances. As a further test of this phenomena, two additional comparison experiments were conducted with a collidine-chemisorbed sample C−MCM-22(33) and a sample containing an intermediate level of physisorbed collidine. The former is the same sample as described above. The latter, denoted as P90−HMCM-22-(33), was prepared by heating collidine-sorbed HMCM-22(33) at 90 °C in dry N_2 until no further weight loss is observed; on this material again, both chemisorbed collidine as well as

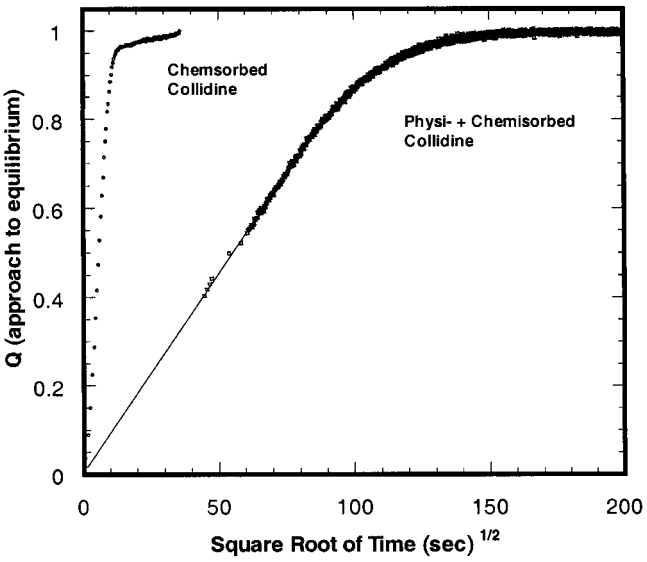

Figure 8. 3-Methylpentane sorption on (a) C−HMCM-22(33), containing chemisorbed collidine, and (b) P−HMCM-22(33), containing physisorbed and chemisorbed collidine at 30 °C, 35 Torr 3-methylpentane, plotted as Q(approach to equilibrium) as a function of the square root of time ($s^{1/2}$). $Q(\infty)$ values for these two adsorbents are 76.5 and 58.6 mg/g ash, respectively.

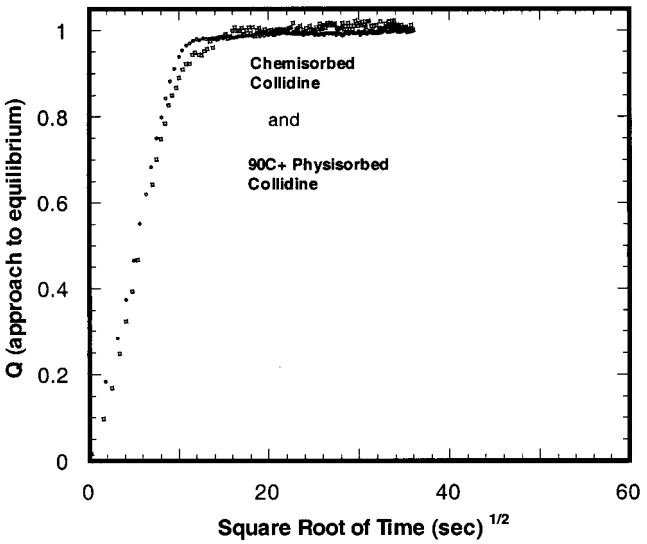

Figure 9. 3-Methylpenetane sorption on (a) C−HMCM-22(33) containing chemisorbed collidine (○), and (b) P90−HMCM-22(33) containing physisorbed plus chemisorbed collidine equilibrated at 90 °C (□), at 35 Torr 3-methylpentane, plotted as Q(approach to equilibrium) as a function of the square root of time ($s^{1/2}$). $Q(\infty)$ values for these two adsorbents are 58.5 and 37.4 mg/g ash, respectively.

physisorbed collidine are present. As can be seen from the sorption results shown in Figure 9, the sorption rate of 3-methylpentane on P90−HMCM-22(33) is similar to that on C−HMCM-22(33), indicating that most of the collidine physisorbed on the pore mouth area causing the pore blockage in the 45 °C pretreated material is removed after 90 °C treatment. This means that the more strongly physisorbed collidine molecules are located in the external pocket area and that these collidine molecules have stronger interaction with the zeolite surface than the collidine molecules adsorbed on the 10-ring pore mouths. It is likely that the physisorbed collidine molecules, surrounded by the zeolite in the surface pockets, have a larger number of van der Waals contacts than the molecules on the "flat" 10-MR pore mouth, producing stronger interactions for the former. In addition, IR results [24,25]show that on the MCM-22 external surface there are nonacidic terminal silanol groups (SiOH) present. Most of the silanol groups are probably situated on the [001] surface since this surface dominates the total external surface area. The interaction of collidine with these nonacidic silanol groups should be stronger than the normal physi-interaction with zeolite surface, but weaker than the chemi-interaction with Brønsted acid sites.

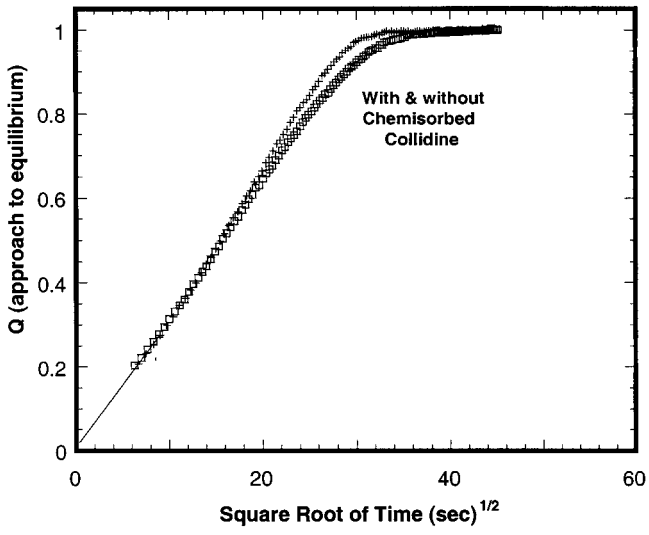

Figure 10. Ethylbenzene adsorption on HMCM-22(33) (+) and C−HMCM-22(33) (□) at 90 °C and 4.1 Torr ethylbenzene pressure plotted as uptake Q(approach to equilibrium) as a function of the square root of time ($s^{1/2}$). $Q(\infty)$ values for these two adsorbents are 100.0 and 65.7 mg/g ash, respectively.

The above results suggest that when collidine-poisoned HMCM-22 is used as a catalyst or sorbent probe at low temperatures, physisorbed collidine on the external surface should be removed with a 200 °C treatment.

Ethylbenzene Synthesis over HMCM-22. HMCM-22 zeolite is very active and selective for ethylbenzene synthesis via the alkylation of benzene with ethylene.[26] Cheng et al. proposed that the Brønsted acid sites on the external surface are the main catalytically active centers[10] on the basis of the following comparison tests: collidine-doped and undoped HMCM-22 were loaded into the reaction systems as catalysts under separate but identical experiments at 220 °C, with the benzene-to-ethylene ratio of 3.5. The undoped HMCM-22 showed very high ethylene conversion (95.6%), while the collidine doped MCM-22 was almost inactive giving only 1.4% conversion. Cheng et al. concluded that the alkylation reaction occurs primarily on the external surface of HMCM-22.[10] Here again, it is of interest to know if collidine molecules block zeolite pore entrances causing the hindered diffusion of reactant (ethylene, benzene) and/or product (ethylbenzene) molecules; the answer bears on arriving at an explanation for the surface-dominated catalysis.

From our previous experimental results, we know that at 220 °C reaction temperature collidine-poisoned HMCM-22 should be free of physisorbed collidine, and chemisorbed collidine left on the sample should not block 10-ring pore openings. This can be confirmed by ethylbenzene adsorption results on HMCM-22(33) and C−HMCM-22(33) shown in Figure 10. The HMCM-22(33) zeolite used for this sorption study is similar to the zeolite used for the benzene alkylation reaction reported by Chen et al.[10] It can be seen that ethylbenzene sorption rate on C−HMCM-22(33) is similar to that on the parent HMCM-22(33), indicating again that collidine molecules chemisorbed on the external surface do not block 10-ring pore mouth entrances. This excludes the possibility that the deactivation of collidine-

poisoned HMCM-22 in alkylation reaction is caused by zeolite pore blockage and supports the primary role of the external surface. The internal acid sites may be inactive due to the formation of polyalkylation products in the supercages limiting the diffusion of reactants and products or simply due to low diffusion rates for these molecules in the intracrystalline channel system compared with the rates on the external surface.[10]

The above reaction results in benzene alkylation with collidine poisoned and collidine free MCM-22 zeolites confirm our assignment of the first step collidine desorption shown in Figure 6a. We assigned this low temperature desorption step to physisorbed collidine. If some chemisorbed collidine were also lost during this step, the collidine-doped zeolite should show some catalytic activity at 220°C reaction temperature. This is not the case. This verified our assignment of the first step collidine desorption to only physisorbed collidine on MCM-22 surface.

Conclusion

Temperature-programmed desorption of ammonia shows that the total amount of Brønsted acid sites in our HMCM-22 zeolite is 0.93 mmol/g, corresponding to a SiO_2/Al_2O_3 ratio of 33. A single ammonia dMeq/dT TPD peak indicates a relatively uniform acid strength of the Brønsted acid sites in HMCM-22(33). The peak maximum at 340 °C indicates that most of the Brønsted acid sites in HMCM-22(33) are strong. Collidine TPD results show that the Brønsted acid sites on the external surface accessible to collidine is 0.108 mmol/g, accounting for 12% of the total Brønsted acid sites. Strong Brønsted acid sites are present on the external surface of MCM-22 zeolite as indicated by the collidine desorption at high temperature. The collidine TPD curve shows distinct desorption steps at 45−200 °C and 200−750 °C, attributed to physisorbed and chemisorbed collidine on the zeolite external surface, respectively. Chemisorbed collidine on the zeolite surface does not influence the sorption rate of 3-methylpantane, indicating that it does not block 10-ring pore mouth openings. This means that collidine can selectively poison the Brønsted acid sites on the MCM-22 zeolite surface without influencing the access to intracrystalline acidic sites. When using collidine-poisoned HMCM-22 in acid catalysis study, physisorbed collidine should be removed by a 200 °C treatment to eliminate the influence of physisorbed collidine. Also, the catalytic reaction temperature should not exceed 200 °C to avoid desorption of chemisorbed collidine. Adsorption experiments also show that collidine poisoning does not influence the sorption rate of ethylbenzene, revealing that the inactivation of collidine-doped HMCM-22 in benzene alkylation reaction is not caused by zeolite pore mouth blocking. This supports the external surface reaction mechanism of MCM-22 zeolite in benzene alkylation with ethylene.

Acknowledgment. We acknowledge and thank the Mobil Technology Company (MTC) for their support of this project. We acknowledge and thank the following Mobil Technology personnel: T. F. Degnan for the MCM-22 material used herein, M. Kalyanaraman for the TEM photographs, and J.G. Santiesteban and J.C. Cheng of MTC and G.H. Kuehl of the University of Pennsylvania for many helpful discussions.

References and Notes

(1) Leonowicz, M. E.; Lawton, J. A.; Lawton, S. L.; Rubin, M. K. *Science* **1994**, *264*, 1910.

(2) Ravishankar, R.; Joshi, P. N.; Tamhankar, S. S.; Sivasanker S.; Shiralkar, V. P. *Adsorp. Sci. Technol.* **1998**, *16* (8), 607.

(3) Prakash, A. M.; Wasowicz, T.; Keven, L. *J. Phys. Chem. B* **1997**, *101*, 1985.

(4) Asensi, A.; Corma, A.; Martínez, A. *J. Catal.* **1996**, *158*, 561.

(5) Ravishankar, R.; Sivasanker, S. *Appl. Catal. A* **1996**, *142*, 47.

(6) Wu, P.; Komatsu, T.; Yashima, T. *Micropor. Mesorpor. Mater*. **1998**, *22*, 343.

(7) Lawton, S. L.; Leonowicz, M. E.; Partridge, R. D.; Chu, P.; Rubin, M. K. *Microporous Mesoporous Mater*. **1998**, *23* (1−2), 109.

(8) Corma, A.; Corell, C.; Pérez-Pariente, J.; Guil, J. M.; Guil-López, R.; Nicolopoulos, S.; Calbet, J.; Vallet-Regi, M. *Zeolites* **1996**, *16*, 7.

(9) Weitkamp, J.; Weip, U.; Ernst, S. Catalysis by Microporous Materials. *Stud. Surf. Sci. Catal*. **1995**, *94*, 363.

(10) Cheng, J. C.; Degnan, T. F.; Beck J. S.; Huang Y. Y.; Kalyanaraman M.; Kowalski J. A.; Loehr C. A.; Mazzone, D. N. *Stud. Surf. Sci. Catal*. **1999**, *121*, 53.

(11) Nicolopoulos, S.; González-Calbet, J. M.; Vallet-Regí, M.; Corma, A., Corell, C., Guil, J. M.; Pérez-Pariente, J. *J. Am. Chem. Soc*. **1995**, *117*, 8947.

(12) Roque-Malherbe, R.; Wendelbo, R.; Mifsud, A.; Corma, A. *J. Phys. Chem. B* **1995**, *99*, 14064.

(13) Corma, A.; Gonzàlez-Alfro, V.; Orchillès A. V. *Appl. Catal. A* **1995**, *129*, 203.

(14) Sastre, G.; Fornes, V.; Corma, A. *J. Phys. Chem. B* **2000**, *104*, 4349.

(15) Page, N. M.; Young, L. B.; Blain, D. A. U.S. Patent 4870038, 1989.

(16) DiGuiseppi, F. T.; Han, S.; Heck, R. H. U.S. Patent 5475181, 1995.

(17) Musa, M.; Pop, E.; Pop, G.; Ganea, R.; Birjega, R.; Musca, G.; Milea, L.; Fota, I. *Heterog. Catal.* **1987**, *6*, 177.

(18) Kerr, G. T. *Thermochim. Acta* **1971**, *3*, 113.

(19) Corma, A.; Grande, M. S.; Gonzalez-Alfaro, V.; Orchilles, A. V. *J. Catal*. **1996**, *159* (2), 375.

(20) Corma, A.; Corell, C.; Martínez, A.; Pérez-Pariente, J. Zeolites and Related Microporous Materials. *Stud. Surf. Sci. Catal*. **1994**, *84*, 859.

(21) Onida, B.; Geobaldo, F.; Testa, F.; Crea, F.; Garrone, E. *Stud. Surf. Sci. Catal.* **2000**, *130*, 2951.

(22) Cao, J.; Xu, W.; Li, W.; Dou, T.; Xie, J. *Ranliao Huaxue Xuebao* **1989**, *17* (3), 255.

(23) Dong, W.; Nie, H.; Xiang, S.; Li, H. *Ranliao Huaxue Xuebao* **1989**, *17* (2), 156.

(24) Corma, A.; Corell, C.; Fornés, V.; Kolodziejski, W.; Pérez-Pariente, J. *Zeolites* **1995**, *15*, 576.

(25) Hunger, M.; Ernst, S.; Steuernagel, S.; Weitkamp, J. *Microporous Mater*. **1996**, *6*, 349.

(26) Corma, A.; Martinez-Soria, V.; Schnoeveld, E. *J. Catal*. **2000**, *192*, 163.